

Non-compact Topological Branes on Conifold

Seungjoon Hyun and Sang-Heon Yi

Department of Physics, College of Science, Yonsei University, Seoul 120-749, Korea

Abstract

We consider non-compact branes in topological string theories on a class of Calabi-Yau spaces including the resolved conifold and its mirror. We compute the amplitudes of the insertion of non-compact Lagrangian branes in the A-model on the resolved conifold in the context of the topological vertex as well as the melting crystal picture. They all agree with each other and also agree with the results from Chern-Simons theory, supporting the large N duality. We find that they obey the Schrödinger equation concerning the wavefunction behavior of the amplitudes. We also compute the amplitudes of the non-compact B-branes in the DV matrix model which arises as a B-model open string field theory on the mirror manifold of the deformed conifold. We take the large N duality to consider the B-model on the mirror of the resolved conifold and concern the wave function behavior of this amplitude. We find appropriate descriptions of non-compact branes in each model which give complete agreements among those amplitudes and clarify the salient features including the role of symmetries toward these agreements.

Email : hyun@phya.yonsei.ac.kr, shyi@phya.yonsei.ac.kr

1 Introduction

Topological strings have been a very interesting test ground for various dualities. These dualities in topological strings give us various relations among them that are seemingly unrelated objects. One of the well-known examples is the mirror symmetry between the two Calabi-Yau threefolds. A model topological string theory on a Calabi-Yau space is equivalent to B-model topological string theory on the mirror Calabi-Yau space and vice versa (see, for a review [1][2][3][4]).

Another relation found recently is the large N duality via geometric transition, which is a topological incarnation of the open-closed duality or AdS/CFT correspondence. The A-model open string field theory on the Calabi-Yau spaces of the form $T M$ with N Lagrangian branes wrapped on M reduces to the $U(N)$ Chem-Simons theory on M [5]. In particular, Chem-Simons theory on S^3 describes the A-model open string theory on the deformed conifold, $T S^3$. Through the geometric transition, it is found to be equivalent to the A-model on the resolved conifold [6][7].

Traditionally the exact computation of correlation functions in the topological A-model was regarded as a difficult one because of the worldsheet instanton contributions. This has been changed greatly at least for the model on non-compact toric Calabi-Yau spaces, by introducing topological vertex [8]. Main idea is that the toric Calabi-Yau space can be regarded as the composition of C^3 's. More concretely, the toric C^3 can be represented by a toric diagram as a trivalent vertex, and toric Calabi-Yau spaces can be constructed diagrammatically by gluing these vertices appropriately. The A-model topological string amplitudes on toric Calabi-Yau spaces can be obtained likewise from the topological vertex, which is the open string amplitude on C^3 for non-compact A-branes at three legs in the toric diagram of C^3 . Along these lines, the vacuum partition function of the A-model on the resolved conifold was reproduced. The computation can be easily generalized to the case when the background contains non-compact Lagrangian A-branes.

Another interesting progress in the A-model has been made from the observation that the partition function of the topological A-model on C^3 is the same as the partition function of three-dimensional melting crystal lying on the positive octant of R^3 [9]. Again this relation seems to be generalized to some toric Calabi-Yau spaces. Indeed the vacuum partition function of the topological A-model on the resolved conifold was shown to be reproduced by considering melting crystal model with an extra wall in one direction [10]. In this melting crystal model, defects play the role of the Lagrangian A-branes. Some computations along this line has been made in [11].

On the other hand, remarkable progress on the computation of the correlation function in the topological B-model has been made as well [12]. These developments came from the realization of the W -algebra governing the correlation functions of the topological B-model on the class of local Calabi-Yau threefolds which is given by

$$uv = H(x; y) : \quad (1.1)$$

The symmetry comes from the holomorphic diagrammism of the Calabi-Yau spaces which preserves the holomorphic three form. All the relevant features of the B-model in this class of local Calabi-Yau threefolds can be obtained from the Riemann surface which satisfies

$$H(x; y) = 0 : \quad (1.2)$$

In this model the non-compact B-brane is identified as a fermion in the Riemann surface.

There is a large N duality in the B-model as well. The B-model on a Calabi-Yau space \mathbb{P} with the u on S^3 cycle is equivalent to the open B-model on N holomorphic branes wrapped on \mathbb{P}^1 in the Calabi-Yau space Y which is related to \mathbb{P} via geometric transition. The B-model open string field theory on Y becomes Dijkgraaf-Vafa (DV) matrix model [13].

All these relations, including the mirror symmetry and the large N transition, among various theories are expected to hold for more general background. Especially, the non-compact branes should play an essential role to establish the full equivalence of those theories. For instance, in the Chem-Simons theory, viewed as an open string field theory, the insertion of the non-compact branes gives the generating functional of the correlation functions of gauge invariant observables, namely knot invariants. It plays the same role in the DV matrix model. In the context of the B-m odel closed strings, the insertion of non-compact B-brane generates the deformations of complex structure. All these indicate that it is essential to include non-compact B-branes to establish the full equivalence among these theories. However, there seems to be some subtleties in the relations among these theories in the presence of non-compact branes. Those subtleties have often been overlooked, without causing problems, in the simple model like topological vertex on C^3 and the B-m odel on the deformed conifold.

In this paper, we revisit the topological string theories with non-compact branes. We consider the A-m odel strings on the resolved conifold and the B-m odel on its mirror manifold as well as the open strings on their large N dual Calabi-Yau spaces. In particular we use the topological vertex formalism to compute the amplitudes of the non-compact Lagrangian brane at the various legs in the toric diagram of the resolved conifold. We also compute the amplitudes of the defect in the melting crystal model. In the B-m odel, we compute the amplitude of non-compact holomorphic brane using the DV matrix model and use the large N duality to identify it as the amplitude of non-compact brane in the B-m odel on the mirror of resolved conifold. In all these computations, along with the known results in Chem-Simons theory, we find the correct identification among various parameters and quantities in these models. We also find how the underlying $SL(2; \mathbb{Z})$ symmetries are realized and related among these models with non-compact branes. These computations show manifestly the wavefunction behavior of the A-m odel amplitude, which seems to be a natural consequence of the mirror symmetry. All these show clearly how the non-compact branes in various models are implemented and how they are connected through the chain of mirror symmetry and the large N duality in the topological string theories. Very recently, a paper [14] appeared which deals with the amplitudes of non-compact branes in the B-m odel on the mirror of resolved conifold using the fermionic formulation in [12]. The results in the present paper along with their work complete all those dualities in the presence of the non-compact branes on the class of toric Calabi-Yau spaces.

The organization of this paper is as follows: In the next section, we review various topological string theories and related models, partly in order to establish the notations and the relations among various parameters in those theories. We also review non-compact branes in the open string field theory on S^3 in the deformed conifold, which play the role of sources in the generating functional of knot invariants in the $U(N)$ Chem-Simons theory on S^3 . In section 3, we describe topological vertex and compute the amplitudes of the non-compact branes at the various legs in the toric diagram of the resolved conifold. In section 4, we describe the melting crystal models and compute the amplitudes of the defects and show that they correspond to the non-compact branes in topological vertex as expected. In section 5, we obtain the B-m odel amplitudes of non-compact branes in the mirror of the resolved conifold from the large N dual DV matrix model. In section 6, we show that all these amplitudes in various models are equivalent obeying the same differential equations as well as the same transformation rules under $SL(2; \mathbb{Z})$. In particular we show the wavefunction behavior of the A-m odel amplitudes confirming the suggestion from the mirror symmetry. Finally we draw some conclusions.

2 Topological string theories and their duals

In this section we review the mirror symmetry which relates the A-model topological string theory on the resolved conifold and the B-model on its mirror Calabi-Yau space. We also review the large N duality which connects the closed topological strings on a Calabi-Yau manifold with the open topological strings on another Calabi-Yau space which is related to the former via the geometric transition. This large N duality relates the A-model topological string theory on the resolved conifold with $U(N)$ Chern-Simons theory on S^3 , which is an open string field theory on the deformed conifold. We also consider the amplitude of non-cocompact branes in the open topological string theories on the deformed conifold. In $U(N)$ Chern-Simons theory on S^3 , which is the open topological A-model on deformed conifold, it appears as a Wilson loop and gives rise to the generating functional of knot invariants.

2.1 The large N duality and the mirror symmetry

In this subsection we explain the large N duality which relates open and closed topological strings on Calabi-Yau (CY) threefolds and the mirror symmetry which relates the A- and B-models.

The large N duality in the A-model topological string theory means that two CY threefold X and X^e is related by the geometric transition while physics on two CY's is identical. As the three cycle S^3 wrapped by a large number N of A-branes in X shrinks down, X becomes a singular CY threefold, and then by blowing up the singular point, two cycle P^1 with RR-ux appears while A-branes on S^3 disappear. As a result of this geometric transition, X becomes another non-singular CY threefold X^e . The claim is that in the large N limit, open topological string theory on A-branes is identical to the closed topological string theory on X^e .

The deformed conifold $X = T^*S^3$ can be described by the complex equation as

$$X ; \quad uv = H(x; y) = xy ; \quad (2.1)$$

where m may be understood as the complex structure modulus and corresponds to the size of three cycle S^3 . We consider A-model topological open strings on N A-branes wrapped on a Lagrangian submanifold S^3 . Then the open topological string field theory on A-branes reduces to the $U(N)$ Chern-Simons theory on S^3 .

According to the geometric transition we may set $m = 0$ and get X^e by blowing up the singular geometry as

$$X^e ; \quad uz = x ; \quad v z^0 = y ; \quad (2.2)$$

where z and z^0 are inhomogeneous coordinates on P^1 and are related by $z^0 = 1/z$. It turns out that X^e is the resolved conifold, $O(-1) \oplus O(-1) \oplus P^1$, which is the total space of rank two vector bundle over P^1 . N A-branes on S^3 are replaced by the RR-ux on P^1 through the geometric transition. According to the large N duality, the closed topological A-model on this resolved conifold is equivalent to the $U(N)$ Chern-Simons theory on S^3 . In the closed string side we have two parameters, the string coupling g_s and the Kähler parameter t , while in the gauge theory side we also have two parameters, the gauge coupling g_{CS}^2 and the rank of gauge group N . In this large N duality, they should be identified as

$$g_s = ig_{CS}^2 \frac{2}{k+N} ; \quad t = g_s N ; \quad (2.3)$$

where g_{CS}^2 is the coupling constant with the finite renormalization effect. Indeed it was shown in [6] that the vacuum partition function of $U(N)$ Chern-Simons theory can be resummed using $\frac{1}{N}$

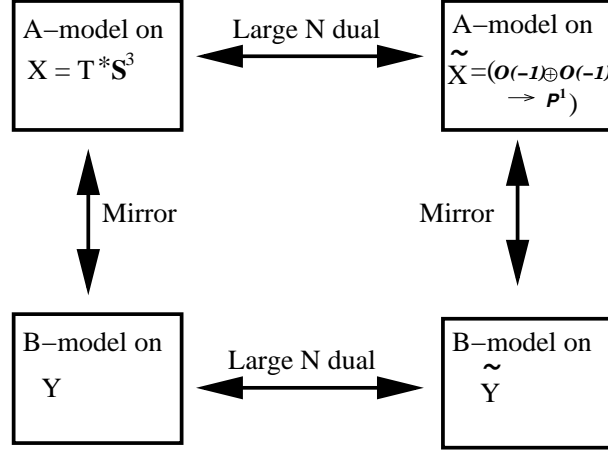


Figure 1: Relations among various models

expansion and shown to be identical with the vacuum partition function of the topological A model on the resolved conifold¹ given by (2.14).

The CY threefold \mathbb{P} mirror to the resolved conifold X^6 can be obtained via a mirror map as shown by Hori and Vafa [16]. For this purpose let us recall the gauged linear sigma model(GLSM) or symplectic quotient description of the resolved conifold [17]

$$X^6; \quad j_1 \bar{j}_1 + j_2 \bar{j}_2 + j_3 \bar{j}_3 + j_4 \bar{j}_4 = \text{Ret } = U(1); \quad (2.4)$$

where $U(1)$ group acts on the coordinates as

$$(j_1; j_2; j_3; j_4) \mapsto (e^{i\theta_1} j_1; e^{i\theta_2} j_2; e^{i\theta_3} j_3; e^{i\theta_4} j_4); \quad (2.5)$$

Variables between two description of the resolved conifolds, X^6 , are related by

$$x = j_1 j_3; \quad y = j_2 j_4; \quad u = j_2 j_3; \quad v = j_1 j_4; \quad z = \frac{1}{z^0} = j_1 j_2; \quad (2.6)$$

The explicit mirror map is given by

$$\text{Ret } Y_i = j_i \bar{j}_i \quad Y_i = e^{Y_i} \quad (2.7)$$

and a Landau-Ginzburg superpotential which characterizes the mirror manifold \mathbb{P} is given by

$$H(y_i) = \sum_i^X y_i; \quad y_1 y_2 = e^{-t} y_3 y_4; \quad (2.8)$$

Note that y_i 's are C variables and the second equation is a constraint coming from GLSM.

One may use the inhomogeneous coordinates to express this curve equation. For example, one may eliminate y_2 using the constraint equation and use C action to set $y_1 = 1$. Introducing variables $x; y$ as $y_3 = e^x; y_4 = e^y$, one get the local CY threefold \mathbb{P} governed by the complex equation

$$uv = H(x; y) = 1 - e^y - e^{-x} + e^{-t - x + y}; \quad (2.9)$$

¹The presence of RR flux doesn't change the partition function of the model [15].

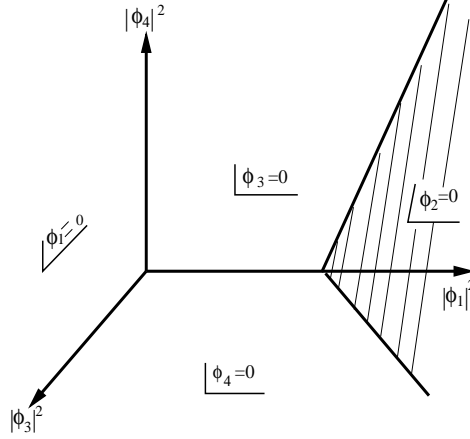


Figure 2: Toric base for the resolved conifold

on which topological B-model strings are equivalent to the topological A-model strings on the resolved conifold X^6 .

Since a linear $SL(2; \mathbb{Z})$ coordinate transformation does not alter the periodicity of x, y and the holomorphic three-form $= dx dy dv = v$, the mirror manifold \mathbb{P} can be alternatively described in terms of new variables x and y

$$\begin{matrix} x \\ y \end{matrix} = \begin{matrix} 1 & 1 \\ 0 & 1 \end{matrix} \begin{matrix} x \\ y \end{matrix} + \begin{matrix} t \\ 0 \end{matrix}; \quad (2.10)$$

with a constant rescaling $e^{x+y} = uv$ as

$$\mathbb{P}; \quad uv = H(x; y) = (e^y - 1)(e^{y+x} - 1) \sim; \quad \sim 1 - e^t; \quad (2.11)$$

where \sim can be interpreted as the complex structure moduli. Note that this geometry is non-singular for $\sim \neq 0$ and contains three cycles.

In this B-model setting one may also consider analogous large N dual B-model open topological strings as in the A-model case, which can be achieved by a geometric transition. Consider the topological B-model on the above Calabi-Yau space with fluxes on S^3 . Now one let the complex structure parameter \sim go to zero and the corresponding three cycle shrinks. Then, new two cycle appears and N B-branes wrapped on this two cycle are dual to the flux on the shrunken three cycle. The manifold Y relevant for this large N dualized B-model strings, which is also mirror to the starting geometry X , is given by the blow-up of the local CY threefold \mathbb{P} with $\sim = 0$ as

$$Y; \quad u z = e^y - 1; \quad v z^0 = e^{y+x} - 1; \quad (2.12)$$

where z and z^0 denote the inhomogeneous coordinates for the blown up P^1 and are related each other by $z^0 = 1/z$. The open string field theory on B-branes wrapped on P^1 reduces to the Dijkgraaf-Vafa matrix model [18].

2.2 The A-model on the resolved conifold

In this section we summarize some relevant results and establish the notations on the A-model topological string theory on the resolved conifold for later use. In general the vacuum partition

function of topological closed strings on a Calabi-Yau manifold² may be written as

$$Z(g_s; t) = \exp [F(g_s; t)] = \exp \sum_{g=0}^{\infty} g_s^{2g-2} F_g(t) ; \quad (2.13)$$

where t denotes Kähler and complex structure moduli for A-model and B-model topological string theory, respectively, and $F_g(t)$ is the genus- g free energy. The topological A-model closed string amplitude on the resolved conifold was obtained by embedding in physical M theory [19]. It is given by³

$$F(g_s; t) = F^{\text{const.}}(g_s) + \sum_{n=1}^{\infty} \frac{1}{n} \frac{e^{nt}}{(2 \sin \frac{ng_s}{2})^2} ; \quad (2.14)$$

where $F^{\text{const.}}(g_s)$ denotes the constant map contribution and t is the Kähler modulus of P^1 . The genus- g free energy for the resolved conifold can be read as

$$F_g(t) = \frac{\frac{1}{2}g}{(2g)!} \sum_{n=1}^{\infty} \frac{e^{nt}}{n^{3-2g}} + F_g^{\text{const.}} ; \quad (2.15)$$

From now on we adopt different conventions and take the partition function of A-model topological strings on the resolved conifold as

$$Z_{X^e}(g_s; t) = \exp [F_{X^e}(g_s; t)] = \exp [F^{\text{const.}}(g_s) + \sum_{n=1}^{\infty} \frac{1}{n} \frac{e^{nt}}{(2 \sinh \frac{ng_s}{2})^2}] ; \quad (2.16)$$

One may regard this convention is coming from the replacement of the weight g_s^{2g-2} by another weight $(-ig_s)^{2g-2}$ such that

$$Z(g_s; t) = \exp [F(g_s; t)] = \exp \sum_{g=0}^{\infty} (-ig_s)^{2g-2} F_g(t) ; \quad (2.17)$$

The explicit form of the constant map contribution on the resolved conifold, $F^{\text{const.}}(g_s)$, is

$$F^{\text{const.}}(g_s) = \sum_{n=1}^{\infty} \frac{1}{n} \frac{1}{(2 \sinh \frac{ng_s}{2})^2} = \ln M(q_c) ; \quad M(q_c) = \prod_{m=1}^{\infty} (1 - q_c^m)^{-m} ; \quad q_c = e^{g_s} = q^{-1} ; \quad (2.18)$$

where $M(q_c)$ is the, so-called, MacMahon function with $\text{Re } g_s > 0$. In the $t \rightarrow 1$ limit, the partition function on resolved conifold reduces to the MacMahon function, thus which is the partition function of topological A-model closed strings on C^3 . For the genus $g=2$, the genus- g free energy may also be written as

$$F_g^{\text{const.}} = (-1)^g \frac{\mathcal{B}_{2g} \mathcal{B}_{2g-2} j}{2g(2g-2)(2g-2)!} = (-1)^g \frac{(X^e)^Z}{2} \frac{1}{M_g} C_{g-1}^3(H) ; \quad g=2 ; \quad (2.19)$$

where \mathcal{B}_{2g} is a Bernoulli number and (X^e) is the Euler characteristic of the CY manifold X^e .

²The topological A-model makes sense on Kähler manifolds.

³Note that there is an ambiguity in the expression for $g=0;1$ coming from the non-compactness of the given CY.

2.3 Non-compact branes in topological A model

The amplitude of non-compact branes can be easily incorporated in the Chem-Simons theory. Our starting set up is A model topological open strings on the deformed conifold $X = T^* S^3$ with a large number N of A-branes wrapped on a Lagrangian submanifold S^3 and another M non-compact A-branes wrapped on a different Lagrangian submanifold $L = R^2 \times S^1$, where these two types of A-branes meet on $S^1 \times S^3$. As alluded in the previous section, after the geometric transition the geometry becomes the resolved conifold, $O(-1) \oplus O(-1) \oplus P^1$. While A-branes on S^3 are replaced by the RR-flux on P^1 in this large N transition, M non-compact A-branes wrapped on L is argued to remain as the Lagrangian A-branes on the resolved conifold X .

In this case the open string field theory on X is reduced to Chem-Simons theories on two three dimensional Lagrangian submanifolds. If we denote the gauge fields on S^3 and $R^2 \times S^1$ as A and A^0 , respectively, then, the effective theory is described by the action

$$S_{CS}[A; S^3] + S_{CS}[A^0; R^2 \times S^1] + S_{int}[\cdot; A; A^0; S^1], \quad (2.20)$$

where S_{CS} denotes the standard Chem-Simons action. The surviving degree of freedom of open topological strings for $S_{int}[S^1]$ is a complex scalar field on the circle which is bi-fundamental in the gauge group $U(N) \times U(M)$. Since $S_{int}[S^1]$ is quadratic in the complex scalar field, we can integrate out and obtain the operator, which was first introduced by Ooguri and Vafa [20],

$$Z(U; V) = \exp \sum_{n=1}^{h_X^1} \frac{1}{n} \text{tr} U^n \text{tr} V^n; \quad (2.21)$$

where ‘tr’ denotes the trace for the fundamental representation and U, V^{-1} are the holonomy matrices around S^1 defined by

$$U = P e^{\int_{S^1} A}; \quad V^{-1} = P e^{\int_{S^1} A^0}; \quad (2.22)$$

Using Frobenius character formula, one can get

$$Z(U; V) = \prod_{i=1}^{h_X^1} \text{Tr} U_i \text{Tr} V_i; \quad (2.23)$$

where Tr_i denotes the trace over an irreducible representation i . Since an irreducible representation for $U(N)$ is one-to-one correspondent with a partition or Young diagram, i is specified by non-decreasing non-negative integers as $i = (f_1, f_2, \dots, f_n)$.

Gauge fields A^0 on non-compact branes can be treated as non-dynamical ones or ‘source’ terms from the viewpoint of $U(N)$ gauge theory on S^3 . Therefore the operator (2.21) may be regarded as a generating functional for Wilson loop observables in all representations

$$hZ(U; V)_{i_{S^3}} = \text{Tr} U_i \text{Tr} V_i; \quad (2.24)$$

This is another example that the string theory leads to a generating functional of field theory naturally. The Wilson loop observable $h\text{Tr} U_i_{S^3}$ was calculated explicitly in [21] for the unknots as

$$h\text{Tr} U_i_{S^3} = \frac{S}{S} = s(q^{\frac{N}{2} - i + \frac{1}{2}}) \dim_q; \quad (2.25)$$

where S is the matrix elements of S -transformation of $SL(2; \mathbb{Z})$ to get S^3 by gluing two solid torus. The function $s(x_i)$ ($i = 1, 2, \dots, N$) is Schur function introduced in the appendix with

some relevant properties, and \dim_q is the, so-called, quantum dimension of the representation, which reduces to the ordinary dimension of the representation in the classical limit $q = e^{g_s} \rightarrow 1$. The concrete expression of (2.25) can be found in the appendix.

Since the orientation is reversed for antibranes, the amplitude for antibrane insertion is given by

$$Z^{-1}(U;V) = \exp \sum_{n=1}^h \frac{1}{n} \text{tr} U^n \text{tr} V^n = (-1)^j \text{Tr}_t U \text{Tr} V; \quad (2.26)$$

which leads to the knot invariants for the unknots

$$hZ^{-1}(U;V)_{S^3} = \sum_{i=1}^X (-1)^j j_{S^3}(q^{\frac{N}{2} - i + \frac{1}{2}}) \text{Tr} V; \quad (2.27)$$

3 Non-compact branes in topological vertex

Topological vertex is the main computational tool for the study of topological Am model on toric Calabi-Yau space [8]. In this section we describe the non-compact branes in the context of topological vertex. Firstly, we describe the topological vertex formalism emphasizing the role of symmetries. We explain the subtleties in the realization of these symmetries through the amplitude. We show this in detail for the case of resolved conifold. Then we consider the insertion of non-compact branes at the external legs in the toric diagram of the resolved conifold, which is believed to be the dual of the non-compact brane configurations in Chern-Simons theory. As will be explained later, this is deeply related to the mirror B model where the amplitude is realized as a wavefunction.

3.1 Topological vertex

The toric diagram of the Calabi-Yau space can be decomposed into the set of vertices which are connected by lines (propagators) [8]. This is basically because each vertex represents C^3 and a toric Calabi-Yau space can be regarded as a union of C^3 in such a way that C action is well-defined globally. The manifold C^3 may be regarded as a total space of T^2 fiber over R^3 , where T^2 fiber space can be taken as the orbit of the following action

$$\begin{aligned} &; (z_1; z_2; z_3) \mapsto (e^{i\theta_1} z_1; z_2; e^{i\theta_2} z_3); \\ &; (z_1; z_2; z_3) \mapsto (e^{i\theta_1} z_1; e^{i\theta_2} z_2; z_3); \end{aligned} \quad (3.1)$$

The moment map for these actions is given by

$$r = \dot{z}_3 \dot{z}_1^* - \dot{z}_1 \dot{z}_3^*; \quad r = \dot{z}_1 \dot{z}_2^* - \dot{z}_2 \dot{z}_1^*; \quad (3.2)$$

The trivalent vertex corresponds to the degeneration locus of T^2 in the R^2 subspace of R^3 base and consists of three edges or legs denoted as two-dimensional vectors $v_i = (p_i; q_i)$, satisfying

$$\sum_{i=1}^3 v_i = 0; \quad (3.3)$$

and

$$v_2 \wedge v_1 = v_1 \wedge v_3 = v_3 \wedge v_2 = 1; \quad (3.4)$$

with the wedge product defined by $v_i \wedge v_j = p_i q_j - q_i p_j$.

Now consider an open string amplitude for this vertex with Lagrangian A-branes attached in all three legs. Then the total open string partition function may be written as

$$Z(V_i) = \sum_{\text{X}} C_{\text{X}} \text{Tr} V_1 \text{Tr} V_2 \text{Tr} V_3; \quad (3.5)$$

where V_i is a source associated to the Lagrangian submanifold at the i -th leg and the summation is taken over all possible irreducible representations. This partition function can be determined from the link invariants of $U(1)$ Chern-Simons theory on S^3 [8]. The explicit expression of the topological vertex amplitude, C_{X} , in terms of Schur function is given in the appendix.

The crucial point is that the topological vertex amplitude which is obtained from the above computations of open string amplitude, corresponds to the closed string amplitude on C^3 with boundaries due to external branes. If we want to find the A-model closed string partition function on C^3 , we simply take the trivial representation for all three legs.

Framing

In the above computations of topological vertex, we used non-compact Lagrangian branes in C^3 . In order to fully specify the model, we need to give the boundary conditions on the fields on these non-compact branes at infinity [22][23][24]. This is called a framing in the topological vertex and corresponds to the framing in the dual Chern-Simons theory. This boundary condition can be specified by modifying the geometry and allowing the T^2 fiber to degenerate at additional locations in the base R^3 so that the Lagrangian branes wrap on compact S^3 cycles. This can be done without affecting the topological A-model amplitudes. Those additional degeneration loci are specified by three vectors f_i satisfying

$$f_i \wedge v_i = 1 : \quad (3.6)$$

It is clear that the above condition is still satisfied with the replacement $f_i = n_i v_i$ for any integer n_i . A framing is the choice of the integers n_i . We choose the framing, $(f_1; f_2; f_3) = (v_2; v_3; v_1)$ as the canonical one and denote all other choices of framing as three numbers n_i relative to this canonical framing.

The topological vertex in the $(n_1; n_2; n_3)$ framing, $C^{n_1 n_2 n_3}$, is related to the topological vertex in the canonical one, C , by the relation:

$$C^{n_1 n_2 n_3} = (-1)^{n_1 j + n_2 j + n_3 j} q^{\frac{1}{2}(n_1 + n_2 + n_3)} C : \quad (3.7)$$

Symmetries

The topological vertex with trivial representation at three legs has $SL(2; \mathbb{Z})$ symmetries inherited from those of T^2 fiber of C^3 . Since the wedge product is invariant under the $SL(2; \mathbb{Z})$ transformation, we can use this $SL(2; \mathbb{Z})$ transformation to change v_i at our disposal. For example, we can permute v_i cyclically and obtain a cyclic symmetry Z_3 . This $SL(2; \mathbb{Z})$ symmetry acts on the vertex amplitude through the replacement:

$$(f_i; v_i) \rightarrow (g \quad f \quad g \quad v) ; \quad g \in SL(2; \mathbb{Z}) \quad (3.8)$$

In what follows, we will consider the $SL(2; \mathbb{Z})$ transformations acting on v_i only,

$$(f_i; v_i) \rightarrow (f_i; \quad g \quad v) ; \quad g \in SL(2; \mathbb{Z}) \quad (3.9)$$

This is in general not a symmetry of the system, thus one should distinguish it from the $SL(2;\mathbb{Z})$ given in (3.8). One may regard this as a passive transformation. One can also consider the active transformation acting f_i only, which moves a non-compact brane at one leg to the one at another leg, while leaving each leg, v_i , invariant. These two viewpoints are connected by the $SL(2;\mathbb{Z})$ symmetry acting on both v_i and f_i as in (3.8).

The topological vertex amplitude C is invariant under the Z_3 subgroup of $SL(2;\mathbb{Z})$ which takes

$$v_1 ! v_2 ; \quad v_2 ! v_3 ; \quad v_3 ! v_1 : \quad (3.10)$$

This Z_3 transformation can be realized as TS^{-1} matrices transforming $v_i = (p_i; q_i)$ as a doublet, where

$$S = \begin{pmatrix} 0 & 1 \\ 1 & 0 \end{pmatrix} ; \quad T = \begin{pmatrix} 1 & 1 \\ 0 & 1 \end{pmatrix} : \quad (3.11)$$

This, in turn, becomes an active ST^{-1} transformation of $SL(2;\mathbb{Z})$ acting on f_i . This results in the cyclic symmetry of the amplitude C .

$$C = C = C : \quad (3.12)$$

The change of framing may also be understood as an active T transformation of $SL(2;\mathbb{Z})$.

The topological vertex for C^3 has also a Z_2 symmetry from the exchange of z_1 and z_2 coordinates of C^3 .

$$C = q^{\frac{1}{2}} (+ + +) C_{\text{t t t}} : \quad (3.13)$$

Note this is not an $SL(2;\mathbb{Z})$ transformation.

Resolved conifold

The whole closed string amplitude of the toric Calabi-Yau space containing more than single vertex can be obtained by gluing appropriately these vertices. The explicit rules for gluing vertices can be found in [8]. For example, the toric diagram for the resolved conifold is given by two vertices connected by a line of length t , Kähler moduli of P^1 .

Using the Schur function representation of the topological vertex given in the appendix, one can easily write the vacuum partition function of the closed string for the resolved conifold as

$$Z^{\text{tv}}(g_s; t) = \sum_{i,j}^X C_{i,j} (e^{t_j})^j C_{i,j} = \sum_{i,j}^X s_i(q) s_j(e^{t_j} q) ; \quad (3.14)$$

where t denotes the transpose of \cdot . It becomes, through the identity of Schur functions given in (A.15),

$$Z^{\text{tv}}(g_s; t) = \prod_{i,j=1}^Y (1 - e^{t_j} q^{i-j+1}) = \exp \sum_{n=0}^X \frac{e^{nt}}{n} \frac{1}{[n]} ; \quad (3.15)$$

where $[n]$ is the so-called q-number defined by

$$[n] = q^{\frac{n}{2}} - q^{-\frac{n}{2}} ; \quad q = e^{g_s} : \quad (3.16)$$

Note that $Z^{\text{tv}}(g_s; t)$ is identical with $Z_{\chi^0}(g_s; t)$ up to the factor $M(q_c)$. This non-existence of $M(q_c)$ is a general feature of the topological vertex calculation and should be taken into account when the corresponding quantities in the dual theories are compared.

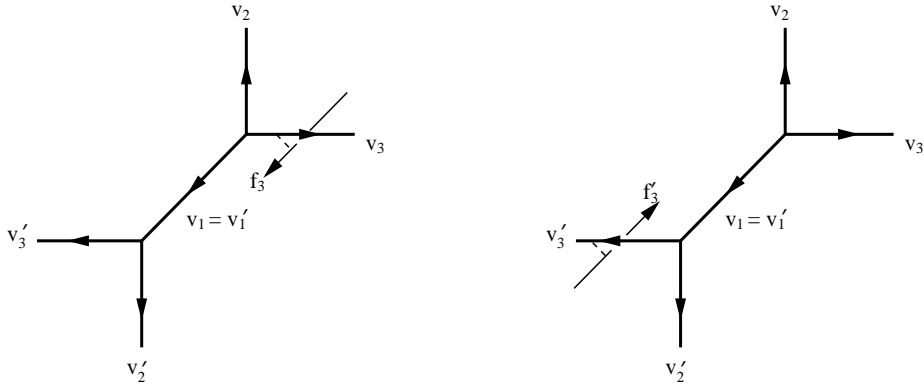


Figure 3: Canonically framed A-branes, f_3 and f_3^0 , on the external legs v_3 and v_3^0

3.2 Non-cocompact branes in the topological vertex

In this section, using topological vertex formalism we compute the amplitudes of non-cocompact branes on the resolved conifold at the various positions.

Branes at an external leg

The amplitude of non-cocompact branes at an external, non-cocompact, leg can be obtained by the replacement

$$C \rightarrow !^X (e^{-r})^{j,j} (-1)^{pj} j q^{\frac{1}{2}p} C = \text{Tr } V ;$$

where p denotes a framing. Therefore the normalized amplitude for \mathbb{Y}_3 A-branes with the framing p at the position \mathbf{r}' on the external leg v_3 in the toric diagram for the resolved conifold, shown in Fig.3, can be calculated in the formalism of topological vertex as

$$\begin{aligned} Z_A^{f_3}(V; r; p) &= \frac{1}{Z^{tv}(g_s; t)} \sum_{j,j} (e^{-r})^{j,j} (-1)^{pj} j q^{\frac{1}{2}p} C = \sum_t (e^{-t})^{j,j} C = \text{Tr } V \\ &= \frac{1}{Z^{tv}} \sum_{j,j} e^{-rj} j (-1)^{pj} j q^{\frac{1}{2}(p+1)} \sum_{s,t} s_t (e^{-t} q) s_{t+} (q) s_{t-} (q) = (q) \text{Tr } V \end{aligned} \quad (3.17)$$

where we used Eqs (A.18) for $C = C$ and Z^{tv} denotes the vacuum partition function of A-model topological strings on the resolved conifold given in (3.15). Using the identities for Schur functions given in Eq. (A.15) and Eq. (A.17), we obtain

$$\begin{aligned} Z_A^{f_3}(V; r; p) &= \sum_{j,j} e^{-rj} j (-1)^{pj} j q^{\frac{1}{2}(p+1)} \sum_{s,t} s_{t+} (q) s_{t-} (e^{-t} q) \text{Tr } V \\ &= \sum_{j,j} (-1)^{j,j} e^{-rj} t_j (-1)^{(p+1)j} t_j q^{(p+1)\frac{t}{2}} q^{\frac{N}{2}j} s_{t+} (q^{\frac{N}{2}-j+\frac{1}{2}}) \text{Tr } V ; \end{aligned} \quad (3.18)$$

using $t = j$, $j = j^t j$ and $t = g_s N$. Note that the amplitude of non-cocompact branes on the external leg v_3^0

$$Z_A^{f_3^0}(V; r; p) = \frac{1}{Z^{tv}} \sum_{j,j} (e^{-r})^{j,j} (-1)^{pj} j q^{\frac{1}{2}p} C = \sum_t (e^{-t})^{j,j} C = \text{Tr } V ; \quad (3.19)$$

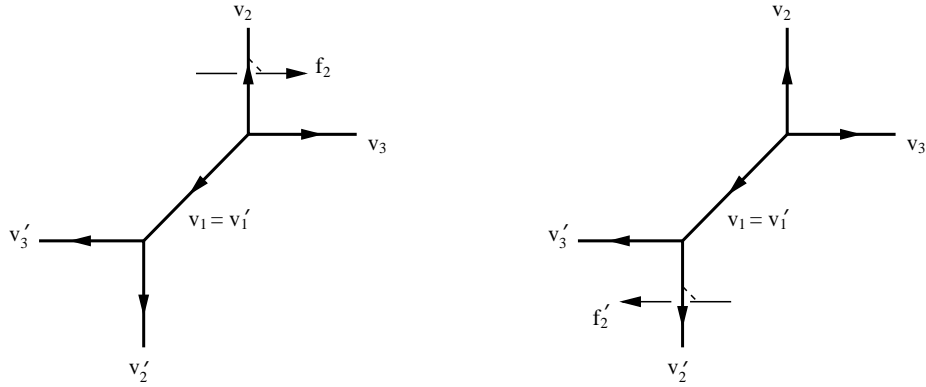


Figure 4: Canonically framed A-branes, f_2 and f_2^0 , on the external legs v_2 and v_2^0

is completely identical with the above Z^{f_3} because of the symmetry of the topological vertex. Henceforth, it is enough to consider only one case.

Antibranes can be obtained by the orientation reversal of branes, which can be achieved by $v_i \rightarrow -v_i$. Therefore the amplitude of antibranes at the position \mathbf{r}' on the external leg v_3 is given by

$$\begin{aligned} Z_A^{f_3}(V; r; p) &= \frac{1}{Z^{tr}} \sum_{X} e^{-r^j j^X} (-1)^{p^j t^j} q^{\frac{1}{2} p^j} (-1)^{j^j} C_{t^j} (e^{t^j})^j C_{t^j} \text{Tr } V \\ &= \sum_{X} e^{-r^j j^X} (-1)^{(p+1)^j j^X} q^{(p+1)\frac{N}{2}} q^{\frac{N}{2} j^j} s_{(q^{\frac{N}{2}})^{j^j}} \text{Tr } V : \end{aligned} \quad (3.20)$$

In contrary to C^3 case, in which the amplitudes for branes and antibranes at the same leg are related by the framing change, the amplitudes for branes and antibranes are completely different in the resolved conifold case.

On the other hand the amplitudes for the (anti) A-branes at the external leg v_2 or v_2^0 shown in Fig. 4 are computed as

$$\begin{aligned} Z_A^{f_2}(V; r; p) &= \frac{1}{Z^{tr}} \sum_{X} (e^{-r^j j^X}) (-1)^{p^j j^X} q^{\frac{1}{2} p^j} C_{t^j} (e^{t^j})^j C_{t^j} \text{Tr } V \\ &= \sum_{X} e^{-r^j j^X} (-1)^{p^j j^X} q^{\frac{N}{2} j^j} s_{(q^{\frac{N}{2}})^{j^j}} \text{Tr } V ; \end{aligned} \quad (3.21)$$

and

$$Z_A^{f_2^0}(V; r; p) = \sum_{X} (-1)^{j^j} e^{-r^j t^j} (-1)^{p^j t^j} q^{\frac{N}{2} j^j} s_{(q^{\frac{N}{2}})^{j^j}} \text{Tr } V ; \quad (3.22)$$

respectively. Note that there are relations between amplitudes of (anti) A-branes at the external legs v_2 and v_3 such that

$$Z_A^{f_2}(V; r; p) = Z_A^{f_3}(V; r; p-1); \quad Z_A^{f_2^0}(V; r; p) = Z_A^{f_3}(V; r; p-1); \quad (3.23)$$

In general we don't expect any relation between branes and antibranes. However, for the resolved conifold, there is a Z_2 symmetry on the geometry exchanging two external legs, and this symmetry is realized as the above relations between amplitudes of branes and antibranes. It is the same

symmetry which exists in C^3 case, alluded earlier in (3.13). As we will see, this aspect will be realized in the mirror B-model setup in the next section, through the wavefunction behavior of the amplitudes under Z_2 .

Special cases of the branes at an external leg

For a single (anti-)brane, the holonomy for 'source' V is given one-dimensional matrix as $V = e^i$, since the gauge group is $U(1)$. Then, by combining with this Wilson line, the position modulus r becomes complexified one, $x = r + i$. Furthermore, representations for $U(1)$ correspond to single row Young diagrams. As a result, the amplitudes for a single brane and antibrane become

$$Z_A^{f_3}(x; p) = Z_A^{f_2}(x; p=1) = \sum_{n=0}^{N-1} q^{\frac{n}{2}(N-(p+1)(n-1))} (-1)^{pn} e^{xn}; \quad (3.24)$$

$$Z_A^{f_3}(x; p) = Z_A^{f_2}(x; p=1) = \sum_{n=0}^{N-1} q^{\frac{n}{2}(N+(p+1)(n-1))} (-1)^{(p+1)n} e^{xn}; \quad (3.25)$$

where $\frac{N+n-1}{n}$ and $\frac{N}{n}$ denote quantum dimensions for a single row and a single column representation. These are explicitly given by

$$\frac{N}{n} \frac{[N]!}{[n]![N-n]!} = q^{\frac{N}{2}n} h_n(q^{\frac{1}{2}}; q^{\frac{3}{2}}; \frac{N}{2}; q^{\frac{1}{2}});$$

$$\frac{N+n-1}{n} \frac{[N+n-1]!}{[n]![N-1]!} = q^{\frac{N}{2}n} e_n(q^{\frac{1}{2}}; q^{\frac{3}{2}}; \frac{N}{2}; q^{\frac{1}{2}});$$

where h_n and e_n are completely symmetric functions and elementary symmetric functions, respectively, related to Schur functions as (A.2) and

$$[n]! \quad [n][n-1] \quad [1]; \quad [0] \quad 1;$$

Note that

$$\sum_{n=1}^N (1 - q^{(n+N-1)})^{-1} = \sum_{n=0}^{N-1} q^{n(N-1+\frac{1}{2})} h_n(q^{\frac{1}{2}}; q^{\frac{3}{2}}; \frac{N}{2}; q^{\frac{1}{2}}); \quad (3.26)$$

and

$$\sum_{n=1}^N (1 - q^{(n+N-1)}) = \sum_{n=0}^{N-1} q^{n(N-1+\frac{1}{2})} (-1)^n e_n(q^{\frac{1}{2}}; q^{\frac{3}{2}}; \frac{N}{2}; q^{\frac{1}{2}}); \quad (3.27)$$

By taking $N \rightarrow 1$ limit, we can reproduce the (anti-)brane amplitudes on C^3 . Note that in the C^3 case brane amplitudes at framing p are identical with antibrane amplitudes at framing $p=1$ in the same leg due to the combination of Z_2 and Z_3 symmetry of C^3 .

In a particular framing, these single (anti-)brane amplitudes can be represented as product forms as

$$Z_A^{f_3}(x; p=1) = Z_A^{f_2}(x; p=0) = \prod_{n=1}^N (1 - e^x q^{n+\frac{1}{2}});$$

$$Z_A^{f_3}(x; p=1) = Z_A^{f_2}(x; p=0) = \prod_{n=1}^N (1 - e^x q^{n+\frac{1}{2}})^{-1}; \quad (3.28)$$

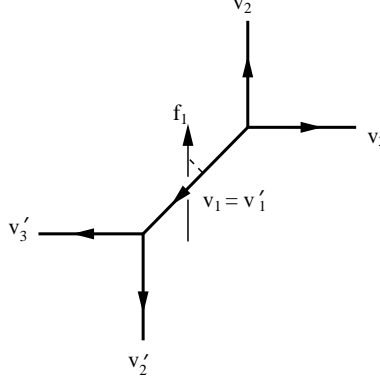


Figure 5: Canonically framed A-branes, f_1 on the internal leg v_1

These forms are relevant for the comparison with the results from melting crystal picture as will be shown in the next section.

Branes at an internal leg

Now let us consider non-compact branes, f_1 , on the internal compact leg, $v_1 = v_1^0$, of the toric diagram for the resolved conifold in Fig. 5. In this case, we consider M stacks of a single (anti-)brane with zero framing, to compare with the results in melting crystal picture. The amplitude of M stacks of a single brane on the compact leg at the position r_a , $a = 1, \dots, M$ with zero framing is

$$\begin{aligned} Z_A^{f_1}(r_a) &= \frac{1}{Z^{tv}} \sum_{a=1}^M C_a (e^{-t})^j e^{\sum_{a=1}^M (r_a j_a j + (t-r_a) j_a j)} C_a \sum_{a=1}^M \text{Tr}_a V_a \text{Tr}_a V_a^{-1} \\ &= \sum_{a=1}^M s_a (e^{r_a q}) s_a (e^{(t-r_a) q}) \text{Tr}_a V_a \text{Tr}_a V_a^{-1} : \end{aligned} \quad (3.29)$$

Again we can complexify the position modulus $x = r + i$ by including the Wilson line $V = e^{i}$ and obtain the amplitude of a single brane as

$$Z_A^{f_1}(x) = \sum_{m,n=0}^{\infty} e^{mx} h_m(q) e^{n(t-x)} h_n(q) = \sum_{m=1}^{\infty} (1 - e^{x} q^{m+\frac{1}{2}})^{-1} \sum_{n=1}^{\infty} (1 - e^{(t-x)} q^{n+\frac{1}{2}})^{-1} : \quad (3.30)$$

Similarly, the amplitude of M stacks of a single antibrane on the compact leg with zero framing at the position r_a is

$$\begin{aligned} Z_A^{f_1}(r_a) &= \frac{1}{Z^{tv}} \sum_{a=1}^M C_a (e^{-t})^j C_a \sum_{a=1}^M (-1)^{j_a j + j_a j} e^{r_a j_a j + (t-r_a) j_a j} \text{Tr}_a V \text{Tr}_a V^{-1} \\ &= \sum_{a=1}^M s_a (e^{r_a q}) s_a (e^{(t-r_a) q}) \text{Tr}_a V \text{Tr}_a V^{-1} : \end{aligned} \quad (3.31)$$

After the same complexification of the position modulus, the amplitude of an antibrane becomes

$$Z_A^{f_1}(x) = \prod_{m,n=0}^{\infty} e^{m x} e_m(-q) e^{n(t-x)} e_n(-q) = \prod_{m=1}^{\infty} (1 - e^{x} q^{m+\frac{1}{2}})^{\frac{1}{2}} \prod_{n=1}^{\infty} (1 - e^{(t-x)} q^{m+\frac{1}{2}})^{\frac{1}{2}} : \quad (3.32)$$

All these branes irrespectively to the internal or external leg insertions have the natural limit to C^3 case by sending $R \rightarrow 0$ ($N \rightarrow \infty$) ! 1. Topological Amodel on C^3 open string partition functions with A-brane with zero framing⁴ with inserted at the position ' r ' can be written as

$$Z(g_s; r) e^{F(g_s; r)} = \exp \prod_{n=1}^{\infty} \frac{1}{n} \frac{e^{nr}}{2 \sinh(\frac{n g_s}{2})} = \exp \prod_{n=1}^{\infty} \frac{1}{n} \frac{e^{nr}}{[n]} = \prod_{k=1}^{\infty} (1 - e^r q^{n+\frac{1}{2}})^{-1} : \quad (3.33)$$

4 Effects in the melting crystal model

In this section we consider the melting crystal model [9] which seems to be the another realization of the topological Amodel. In particular we consider (anti-)defects in the melting crystal model which corresponds to the non-compact branes in the topological Amodel on the resolved conifold [11]. Since these defects were considered recently in [25], we will be brief and present main results which clearly show the correspondence with the topological Amodel.

As noted earlier, the vacuum partition function of the topological Amodel closed strings on C^3 is given by eq. (2.18). This is identical with the partition function of the melting crystal of cubic lattice in the positive octant of R^3 ,

$$Z_{\text{crystal}}(q_c) = \prod_{\substack{\text{3d partition} \\ \text{X}}}^{q_c^{\# \text{ boxes}}} ; \quad (4.1)$$

where $q_c = e^{g_s}$. This observation led to the conjecture that there exists more general melting crystal picture for topological Amodel strings on toric Calabi-Yau spaces.

The 3d partition can be regarded as the composition of 2d partitions satisfying the, so-called, interlacing conditions. Conversely speaking, 2d partitions satisfying the interlacing condition appear as slicings of the 3d partition. This is clear from the equivalence between the partition and Young diagrams. However, this decomposition of the 3d partition into 2d partitions is not unique. We will adopt the convention in which the diagonal slicing is given by $y = x$ on the positive octant $(x; y; z) \in R^3_+$.

Two dimensional Young diagram can be represented in terms of a fermionic Fock space. In the transformatrix formalism, we adopt this and assign a fermionic Fock space to each two dimensional partition. In this formalism we introduce the operators which satisfy the relations

$${}_{+}(z) \quad (z^0) = \frac{1}{1 - z^{-1}} \quad (z^0) {}_{+}(z) ; \quad {}_{+}(z) \quad {}^{-1}(z^0) = 1 - \frac{z}{z^0} \quad {}^{-1}(z^0) {}_{+}(z) : \quad (4.2)$$

These operators can be realized in terms of a simple harmonic oscillators $_{\text{m}}$, which are modes of the bosonization of the fermions, as ${}_{+}(z) = \exp \left[\sum_{n=1}^{\infty} \frac{1}{n} z^n \right]$ and ${}_{-}(z) = \exp \left[\sum_{n=1}^{\infty} \frac{1}{n} z^{-n} \right]$ with $[_{\text{m}}; _n] = \delta_{\text{m}, \text{n}} \delta_{\text{m}+\text{n}, 0}$.

A melting crystal model for the resolved conifold X^6 is suggested [10] as the lattice in units of g_s in the positive octant R^3_+ with one wall, for example, at the position $y = g_s N$, see Fig. 6. The

⁴This is equivalent with antiA-brane with $p = -1$ framing.

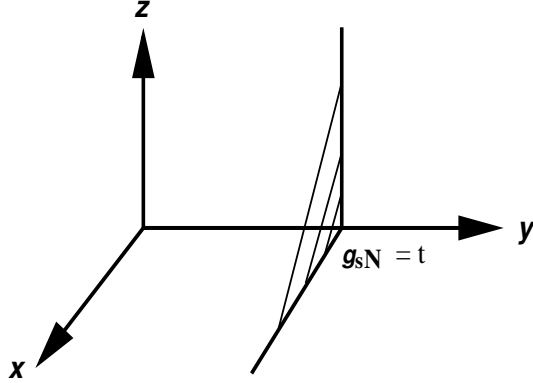


Figure 6: melting crystal model for the resolved conifold

partition function of this melting crystal model is given by

$$Z^{\text{crystal}}(N; q_c) = \sum_{n=1}^D \frac{q_c^n}{(q_c^{n+1})} + \sum_{m=1}^E \frac{q_c^m}{(q_c^{m+1})} = M(q_c) \sum_{n=1}^D (1 - q_c^{n+N})^n : \quad (4.3)$$

One may recall $q_c = q^{-1}$ to see that the partition function is identical with $Z_{\mathcal{X}}(g_s; t)$ in (2.16) by performing a resummation and setting $g_s N = t$. In this melting crystal model, the length from the origin to the wall at the position $y = g_s N$ corresponds to the Kähler moduli of the resolved conifold. This suggests that x -axis and y -axis may correspond to the external and internal leg, respectively, of toric diagram for the resolved conifold \mathcal{X} .

D effects

A defect in the melting crystal model corresponds to a single non-cocompact A-brane in the topological A-model. D effect and anti-defect operators in melting crystals are introduced as certain fermionic operators

$$D(z) = \frac{1}{z} (z) + (z); \quad D(z) = (z) + \frac{1}{z} (z) : \quad (4.4)$$

The partition function with one defect on the x -axis at the position $x = g_s(N_1 + 1/2)$ is given by inserting $D(z = q_c^{N_1 + 1/2})$ at the appropriate position as,

$$Z_D(N_1; N; q_c) = \sum_{n=N_1+2}^D \frac{q_c^n}{(q_c^{n+1/2})} + D(q_c^{N_1 + 1/2}) \sum_{n=1}^{N_1+1} \frac{q_c^n}{(q_c^{n+1/2})} + \sum_{m=1}^E \frac{q_c^m}{(q_c^{m+1/2})} = 0 : \quad (4.5)$$

Using the commutation relations between 's we obtain

$$Z_D(N_1; N; q_c) = [(q_c)]^1 Z^{\text{crystal}}(N; q_c) \sum_{n=1}^D \frac{1}{1 - q_c^{n+N_1}} : \quad (4.6)$$

where $[(q_c)]^1 = \prod_{n=1}^Q (1 - q_c^n)$. After normalizing by $[(q_c)]^1 Z^{\text{crystal}}(N; q_c)$, the amplitude of a defect on the x -axis at $x = g_s(N_1 + 1/2)$ becomes identical with the amplitude, given in eq. (3.28), of

a non-cocompact brane with $p = 0$ at the external leg v_2 (also v_2^0) with the complexified modulus $x = g_s (N_1 + 1=2)$ in the toric diagram of the resolved conifold, see Fig. 4.

It is straightforward, following the argument of the C^3 case in [11], to get the normalized amplitude for d defects as

$$Z_D^{\text{norm}}(N_i; q_c) = \prod_{1 \leq i < j \leq d} \left(1 - q_c^{N_j - N_i}\right) \prod_{i=1}^d \frac{1}{1 - q_c^{n+N_i}}; \quad (4.7)$$

with $N_i < N_j$ for $i < j$.

The amplitude for an anti-defect at x -axis can be obtained by inserting $z_D (q_c^{N_1 + 1=2})$ instead and is given by

$$Z_D(N_1; N; q_c) = \prod_{n=1}^N \left(1 - q_c^{n+N_1}\right); \quad (4.8)$$

The normalized amplitude of anti-defect is identical with the amplitude of a non-cocompact anti-brane with $p = 0$ at the external leg v_2 (also v_2^0) in the toric diagram of the resolved conifold. The normalized amplitude of multi anti-defects at x -axis can be computed in the similar fashion as in the multi defect case and is given by

$$Z_D^{\text{norm}}(N_i; q_c) = \prod_{1 \leq i < j \leq d} \left(1 - q_c^{N_j - N_i}\right) \prod_{i=1}^d \frac{1}{1 - q_c^{n+N_i}}; \quad (4.9)$$

A couple of comments are in order for the amplitude of (anti-)defects inserted on the y -axis. First of all, when we use the formula for z_D and z , (4.4), z is determined by the slicing one takes. We use different z for the defect on the y -axis from z for the defect on the x -axis, which are inverse to each other and are due to the diagonal slicing. Secondly, since the insertion of (anti-)defects on the y -axis corresponds to (anti-)branes in the topological A model inserted at P^1 , we generally expect the change of Kähler parameter of P^1 , and it appears as the shift of the position of the wall in the melting crystal model [10][25].

We would like to emphasize that, as will be shown below, the defect on the y -axis corresponds to the anti-brane with $p = 0$ at the compact leg v_1 in the toric diagram of the resolved conifold. This implies that we should interchange the name of defect and anti-defect operators defined on y -axis if we want to have the correspondence of the naming of brane/anti-brane with $p = 0$ in topological vertex with defect/anti-defect, independent of the inserted axis. In the case of C^3 , it was not clear since the amplitude of the non-cocompact brane with $p = 1$ is the same as the amplitude of the non-cocompact anti-brane with $p = 0$ due to Z_2 and Z_3 symmetries. By considering more general space, we can identify the correct defect/anti-defect operators corresponding to the brane/anti-brane operators, respectively, independent of the position where they are inserted. In this paper we follow the earlier literatures and use the convention shown in (4.4).

The amplitude of the defect insertion on the y -axis at the position $y = g_s (N_1 + 1=2)$ can be computed by inserting $z_D (z = q_c^{N_1 + 1=2})$ at the appropriate position can be written as

$$Z_D(N_1; N; q_c) = 0 \prod_{n=1}^{\frac{N}{2}} \left(1 - q_c^{n - \frac{1}{2}}\right) \prod_{m=1}^{\frac{N}{2}+1} \left(q_c^{m + \frac{1}{2}}\right) z_D \left(q_c^{N_1 - \frac{1}{2}}\right) \prod_{m=N_1+2}^{\frac{N}{2}+1} \left(q_c^{m + \frac{1}{2}}\right) 0 \quad (4.10)$$

and the normalized amplitude becomes

$$Z_D^{\text{norm}}(N_1; N; q_c) = \prod_{m=1}^{\frac{Y}{2}} (1 - q_c^{m+N_1}) \prod_{n=1}^{\frac{Y}{2}} (1 - q_c^{n+N-N_1}) : \quad (4.11)$$

As was mentioned earlier, this corresponds to the topological vertex amplitude (3.30) of the non-compact anti-branes with $p = 0$ inserted at the compact leg v_1 in the toric diagram of the resolved conifold. Similarly, we can compute the normalized amplitude of the anti-defect insertion on the y -axis at the position $y = g_s(N_1 + 1/2)$ and find

$$Z_D^{\text{norm}}(N_1; N; q_c) = \prod_{m=1}^{\frac{Y}{2}} (1 - q_c^{m+N_1})^{-1} \prod_{n=1}^{\frac{Y}{2}} (1 - q_c^{n+N-N_1})^{-1} : \quad (4.12)$$

This in turn corresponds to the amplitude of the non-compact brane inserted at v_1 leg with $p = 0$. It is straightforward to generalize those in the above to the amplitude of multi-(anti-)defects insertion at y -axis as shown in the case of those at x -axis and is omitted.

5 The B-m odel on the m irror of resolved conifold

In this section we consider the B-m odel topological string theory on the m irror space of the resolved conifold. At the beginning we review some salient features of the B-m odel on some class of the Calabi-Yau spaces. Then we compute the amplitudes of non-compact brane insertion in the open topological B-m odel on the m irror space of deformed conifold in the context of DV m atrix m odel. We regard those as the amplitudes of non-compact branes in the topological B-m odel on the m irror space of resolved conifold using the large N duality. We show that they satisfy the Schrodinger wave equation confirming the wavefunction nature of the amplitude in the B-m odel topological string theory.

5.1 The B-m odel

The topological B-m odel on the Calabi-Yau space gives the informations on the complex structure moduli space. The symmetries of the B-m odel on the Calabi-Yau space involve holomorphic diffeomorphisms which preserve the curve equation, like (2.11), and the holomorphic 3-form

$$= \frac{1}{4^{-2}} \frac{dx \wedge dy \wedge du}{u} : \quad (5.1)$$

The Calabi-Yau geometry characterized by the curve equation of the form

$$uv = H(x; y) \quad (5.2)$$

can be regarded as a bration over the $(x; y)$ plane with one dimensional fibers. The surface satisfying

$$H(x; y) = 0 \quad (5.3)$$

in the base manifold is the locus where the fiber degenerates into two components $u = 0$ and $v = 0$. It was shown in [12] that this type of CY geometry is characterized by the algebraic curve (5.3) and the complex deformations of the CY are captured by the canonical one-form, $\omega = ydx$. Therefore if one considers the deformation of the function $H(x; y)$, while keeping $u; v$ fixed, the

target space theory of B-m odel, namely Kodaira-Spencer theory, essentially reduces to the one on the Riemann surface (5.3). The Kodaira-Spencer field is related to the one form $\theta = \theta$ by $\theta = \theta$. When restricted to the Riemann surface (5.3), they become the symplectic diffeomorphisms which preserve the equation (5.3) and symplectic two-form $dx \wedge dy$ of the base manifold. In the quantum Kodaira-Spencer theory, they are realized as the W-algebra symmetry.

The Riemann surface satisfying $H(y_i) = 0$ in (2.8) is a genus 0 surface, i.e. a sphere, with four boundaries or punctures. Near each puncture we can choose a local coordinate x and its conjugate pair y such that $x \neq 1$ and $y \neq 0$ at the puncture (see, for example, the discussion leading (2.9)). Since the complex deformations of the Riemann sphere can arise only at the boundaries, it is enough to consider the deformation generated by the insertion of non-compact B-branes near the punctures. Since $(x; y)$ is a symplectic pair in the geometry and, furthermore, the action of non-compact B-branes near the x -patch is given by

$$S_B = \frac{1}{g_s} \int_Z y \partial_x ; \quad (5.4)$$

y naturally plays the role of conjugate momentum of x in the quantization of branes with the commutation relations

$$[y; x] = g_s : \quad (5.5)$$

As noted in the above, this conjugate pair is deeply related to the Kodaira-Spencer field through the one-form $\theta = ydx = \theta$.

Similarly, one can assign an appropriate coordinate and its conjugate momentum near each patch. The non-compact brane near one patch can be moved around and can be connected with the one in another patch by the $SL(2; \mathbb{Z})$ coordinate transformations. This $SL(2; \mathbb{Z})$ transformation is the symplectic diffeomorphism which preserves the symplectic two form $dx \wedge dy$ and the periodicity of the coordinates $x; y$. There is also freedom in the choice of $(x; y)$, in particular, coordinate transformation of the form

$$x \mapsto x + ny; \quad y \mapsto y ;$$

where n is an arbitrary integer. This is also a part of the symplectic diffeomorphism, $SL(2; \mathbb{Z})$ and is called a framing in the B-m odel. As will be clear, it is closely related to the framing in the mirror topological A-m odel or topological vertex.

In the case of antibranes, the action becomes the minus of the action of branes, $S_B = -S_B$, and thus, in the quantization, the conjugate momentum of x becomes $-y$ which results in the commutation relation, $[y; x] = -g_s$.

5.2 Non-compact branes in topological B-m odel

Non-compact B-branes inserted near a puncture in the Riemann surface are described by free chiral fermions [8] which is related to the Kodaira-Spencer field by $(x) = \exp(-\theta(x) = g_s)$. In general, the B-m odel amplitudes behave as a wavefunction [26]. In particular, one-point function of a fermion which corresponds to the amplitude of single non-compact brane insertion should satisfy the Schrodinger equation whose Hamiltonian is given by the equation of the Riemann surface [12]:

$$H(x; y = g_s \theta(x)) h(x)i = 0 : \quad (5.6)$$

The anti-chiral fermion corresponding to an anti-brane can be represented by $(x) = \exp(-\theta(x) = g_s)$ and satisfies

$$H(x; y = -g_s \theta(x)) h(x)i = 0 : \quad (5.7)$$

Instead of obtaining the one-point function of a fermion directly from the closed B-m odel, we consider the amplitude of the non-cou n pact brane in the context of the large N dual open B-m odel on Y , which is also the m irror of the deformed conifold. For this purpose it is convenient to use the coordinate transformation alluded earlier in section 2.1 and use the curve equation $H(x; y) = 0$ in eq.(2.11) and take the geometric transition.

The resultant open string field theory reduces to DV m atrix m odel with the partition function

$$Z = \frac{1}{\text{vol}(U(N))} \int d_H U \exp \frac{1}{2g_s} \text{Tr} U^2 \quad (5.8)$$

where U is a Hermitian m atrix and the m easure $d_H U$ is the unitary one [18]. When expressed in terms of the diagonal components, the partition function reduces to

$$Z = \int \prod_i du_i \prod_{i < j} \sin^2 \frac{u_i - u_j}{2} \exp \frac{h}{2g_s} \sum_i u_i^2 \quad (5.9)$$

In this large N duality, the non-cou n pact B-branes presumably remain as the non-cou n pact B-branes, meeting the compact one at a point. The surviving degree of freedom of open string m odes connecting these branes is a bi-fundamental complex scalar whose path integral is given by

$$\frac{Z}{D} = \frac{h}{\det(V - 1_N \otimes 1_M \otimes U)} = \det(V - 1_N \otimes 1_M \otimes U)^{-1}; \quad (5.10)$$

where U and V are m atrices from compact and non-cou n pact branes, respectively.

If we consider M non-cou n pact branes at the M different positions as $e^{-v_1}; \dots; e^{-v_M}$ on P^1 , the m atrix V becomes $V = \text{diag}(e^{-v_1}; \dots; e^{-v_M})$ and thus we have

$$\frac{D}{\det(e^{-v_1} \otimes U) \det(e^{-v_2} \otimes U) \dots \det(e^{-v_M} \otimes U)}; \quad (5.11)$$

where the expectation value is taken with respect to U . Therefore the amplitude of a non-cou n pact holomorphic brane is given by $\frac{1}{\det(e^{-v} \otimes U)}$ and using

$$h \text{Tr} U i = q^{\frac{N}{2}} \int q^{-\frac{1}{2}} \text{dim}_q; \quad q = e^{g_s} \quad (5.12)$$

we obtain

$$\frac{D}{\det(e^{-v} \otimes U)} = \sum_{n=0}^{\infty} \frac{1}{q^{\frac{n}{2}(N+n-1)}} (e^v)^{N+n}; \quad (5.13)$$

One may consider this as the amplitude of a non-cou n pact brane in the topological B-m odel on \mathbb{P} through the large N duality

$$h(x)i = \frac{D}{\det(e^x \otimes U)} \quad (5.14)$$

Indeed it satisfies the Schrodinger equation (5.6) where the Hamiltonian, inherited from the curve equation (2.11), is given by

$$H(x; y = g_s \theta_x) = q^N - e^{g_s \theta_x} - q^{\frac{1}{2}} e^x e^{g_s \theta_x} + q^{\frac{1}{2}} e^x e^{2g_s \theta_x}; \quad (5.15)$$

The relevant open string mode connecting the compact brane and the non-compact antibrane is a bi-fundamental complex fermion. Therefore the path integral of the amplitude of the insertion of an antibrane is given by the normalized expectation value of determinants as

$$\text{hdet}(e^{-v} - U)i = \sum_{n=0}^{X^N} q^{\frac{n}{2}(N-n+1)} (-1)^n (e^{-v})^N - ^n : \quad (5.16)$$

The large N dual amplitude $h(x)i = \text{hdet}(e^{-x} - U)i$ satisfies the Schrödinger equation (5.7) with the Hamiltonian

$$H(x; y = g_s \theta_x) = q^N - e^{g_s \theta_x} - q^{\frac{1}{2}} e^x e^{g_s \theta_x} + q^{\frac{1}{2}} e^x e^{2g_s \theta_x} : \quad (5.17)$$

There is a different version of the matrix model⁵ dual to the closed B_R -model [27]. This model is a Hermitean matrix model with logarithmic action whose path integral is given by $\int dM e^{-\frac{1}{2g_s} \text{Tr}(\ln M)^2}$. In this matrix model, the correlation functions of determinants are given by the Slater determinant of orthogonal polynomials. In the case at hand, the relevant orthogonal polynomials are known as Stieltjes-Wigert ones. In particular, the matrix model vacuum expectation value of an antibrane is

$$\text{hdet}(e^{-x} - M)i = (-1)^N q^{\frac{1}{8}N(N-3)} \sum_{n=0}^{X^N} q^{\frac{n}{2}(n+N)} (-q^{\frac{1}{2}} e^{-x})^n : \quad (5.18)$$

which is identical to $\text{hdet}(e^{-v} - U)i$ with identification $x = v - g_s N$ up to an overall constant factor.

6 Equivalence among various models

In this section we compare the amplitudes of non-compact branes in various models. We find the exact correspondence among the non-compact branes in the topological string theories.

The coordinate patches of Riemann sphere with four punctures

We describe the coordinate patches of Riemann sphere characterized by the curve equation

$$\begin{aligned} e^{Y_1} + e^{Y_2} + e^{Y_3} + e^{Y_4} &= 0 \\ Y_1 + Y_2 &= Y_3 + Y_4 + t \end{aligned} \quad (6.1)$$

in the homogeneous coordinates. It has four boundaries and there is an appropriate coordinate near each boundary.

Introduce the coordinates $u_{i,j}$,

$$\begin{aligned} u_1 &= Y_4 - Y_3 ; & u_2 &= Y_3 - Y_1 ; \\ u_3 &= Y_3 - Y_4 ; & u_4 &= Y_4 - Y_2 ; \end{aligned} \quad (6.2)$$

in which the constraints become

$$u_2 + u_4 + t = 0 ; \quad u_1 + u_3 = 0 : \quad (6.3)$$

Then each boundary patch corresponds to the region where $u_i \neq 1$ and is described by the local coordinate $x_i = u_i + i$, which is the natural 'at' coordinate related to the integrality structure of A_R -model [23]. One can find the canonical conjugate momentum y_i in each coordinate patch by

Table 1: coordinate patches

coordinate x	momentum y	curve
$u_1 + i$	$u_2 + i$	$e^x e^y + e^x e^y t + 1 = 0$
$u_2 + i$	$u_1 u_2 + i$	$e^x e^y + e^{x+y} t + 1 = 0$
$u_3 + i$	$u_4 + i$	$e^x e^y + e^x e^y t + 1 = 0$
$u_4 + i$	$u_3 u_4 + i$	$e^x e^y + e^{x+y} t + 1 = 0$

requiring $y_i \neq 0$ as $x_i \neq 1$. The coordinate and conjugate momentum and the curve equation in each patch are displayed in the table 1.

$SL(2, \mathbb{Z})$ transformation in the Riemann sphere

The coordinate and momentum in each patch are related by $SL(2, \mathbb{Z})$ transformations which preserve the symplectic two form and the periodicity of the coordinates x_i and momenta y_i . The coordinate transformations from u_1 -patch to u_2 and from u_3 -patch to u_4 are given by $SL(2, \mathbb{Z})$ transformation $S^{-1}T$, while the coordinate transformations from u_2 -patch to u_3 and from u_4 -patch to u_1 are given by $T^{-1}S^{-1}$ transformation supplemented by constant shift.

$$\begin{array}{ccccccccc} x_1 & S^{-1}T & x_2 & T^{-1}S^{-1} & x_3 & S^{-1}T & x_4 & T^{-1}S^{-1} & x_1 \\ y_1 & & y_2 & & y_3 & & y_4 & & y_1 \end{array} : \quad (6.4)$$

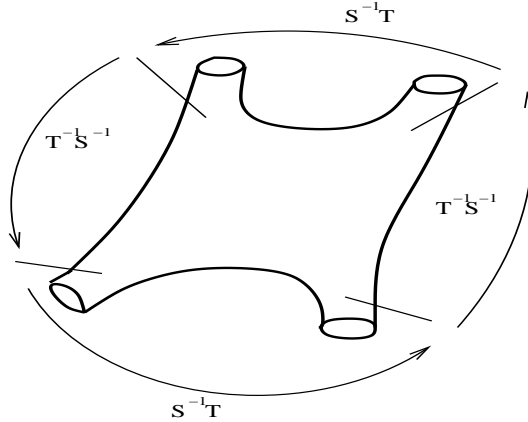


Figure 7: $SL(2, \mathbb{Z})$ transformations relating coordinates among patches in the Riemann surface

$SL(2, \mathbb{Z})$ transformation in the toric diagram

As alluded earlier, the topological vertex also has $SL(2, \mathbb{Z})$ transformations acting on the leg $v_i = (p_i; q_i)$. In the resolved conifold case, these transformation can be considered acting on the

⁵The unitary matrix model version of the above DV matrix model is also obtained in [10].

four external legs $v_{2,3}$ and $v_{2,3}^0$ as

$$p_3 \underset{q_3}{\text{TS}!^1} p_2 \underset{q_2}{\text{S}^1 \text{T}^1} p_3^0 \underset{q_3^0}{\text{TS}!^1} p_4^0 \underset{q_4^0}{\text{S}^1 \text{T}^1} p_3; \quad (6.5)$$

which is exactly in one-to-one correspondence with the transformations in the Riemann sphere, and can be realized, in the active view point, as moving A-branes from one leg to another one as (see, Fig. 8.)

$$f_3 \underset{f_3}{\text{ST}!^1} f_2 \underset{f_2}{\text{T}^1} f_3^0 \underset{f_3^0}{\text{ST}!^1} f_2^0 \underset{f_2^0}{\text{T}^1} f_3; \quad (6.6)$$

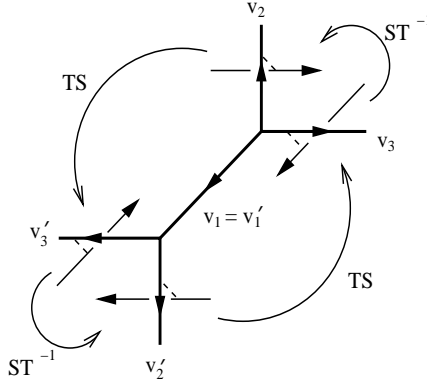


Figure 8: Active $SL(2; \mathbb{Z})$ transformations acting on branes at the external legs in the toric diagram of the resolved conifold, X^E

The correspondence between the transformations of A- and B-models can be easily inferred from the momentum map of the T^2 action for the resolved conifold

$$r(\) = j_4 \hat{j} \quad j_1 \hat{j}; \quad r = j_1 \hat{j} \quad j_3 \hat{j}; \quad (6.7)$$

which can also be written as

$$r(\) = j_2 \hat{j} \quad j_3 \hat{j} \quad \text{Ret}; \quad r = j_4 \hat{j} \quad j_2 \hat{j} + \text{Ret}; \quad (6.8)$$

For example, the coordinate and momentum in the u_1 -patch of the Riemann surface is given by $(x_1; y_1) = (Y_4 - Y_3 + i; Y_3 - Y_1 + i)$ whose real part is nothing but $(r + r; r)$. If the same transformation matrices are applied on $(r + r; r)$ as those on $(x_1; y_1)$, namely $S^{-1}T$, then naturally the transformation matrices for $v_3 = (p_3; q_3)$ leg become TS^{-1} . Therefore one may regard this exact correspondence between the transformation rules of both sides as the consequence of the mirror symmetry between those two Calabi-Yau spaces X^E and \mathbb{P} .

The wavefunction of a non-compact brane and mirror symmetry

We obtained the A-model amplitudes of the non-compact brane inserted at the various external legs of the toric diagram for the resolved conifold in section 3. Now we verify that these amplitudes exactly correspond to the B-model amplitudes of the non-compact brane inserted near the punctures

of the Riemann surface in the mirror manifold of the resolved conifold, thus confirming the mirror symmetry. This can be achieved by showing that the A-model amplitudes satisfy the Schrödinger equation whose Hamiltonian is given by the curve equation $H(x; y) = 0$ with the replacements $y = g_s \theta_x$ for branes and $y = -g_s \theta_x$ for anti-branes.

Essentially there are only two different realizations of the curve equation as is clearly seen in the Table 1. One can see that the brane amplitude at the v_3 leg in the toric diagram for the resolved conifold satisfies

$$1 - e^{g_s \theta_x} - (-1)^p q^{\frac{1}{2}} e^{-x} e^{pg_s \theta_x} + (-1)^p q^{N-\frac{1}{2}} e^{-x} e^{(p+1)g_s \theta_x} Z_A^{f_3}(x; p) = 0; \quad (6.9)$$

This tells us that $Z_A^{f_3}(x; p)$ is exactly the one-point function of the B-model non-coupled brane/fermion operator at the u_1 patch, as it satisfies the Schrödinger equation with the Hamiltonian inherited from the curve equation written in the variables for u_1 patch with a framing p . One can also check that the anti-brane amplitude at the external leg v_3 obeys the same Schrödinger equation

$$1 - e^{g_s \theta_x} - (-1)^p q^{\frac{1}{2}} e^{-x} e^{pg_s \theta_x} + (-1)^p q^{N+\frac{1}{2}} e^{-x} e^{(p+1)g_s \theta_x} Z_A^{f_3}(x; p) = 0; \quad (6.10)$$

where now we replaced $y = -g_s \theta_x$ appropriate for anti-branes. Alternatively, after factoring out differential operators, one can show that it satisfies

$$1 - e^{g_s \theta_x} + (-1)^p q^{\frac{1}{2}} e^{-x} e^{(p+1)g_s \theta_x} - (-1)^p q^{N-\frac{1}{2}} e^{-x} e^{(p+2)g_s \theta_x} Z_A^{f_3}(x; p) = 0; \quad (6.11)$$

The Z_2 symmetry of the resolved conifold, which is realized on the brane amplitude as eq. (3.23) implies that similar differential equations hold for the amplitude of non-coupled A-branes at another legs in the toric diagram for the resolved conifold. For example, it can be deduced from eq. (6.11) that the amplitude of non-coupled A-branes at the external leg v_2 satisfies

$$1 - e^{g_s \theta_x} - (-1)^p q^{\frac{1}{2}} e^{-x} e^{pg_s \theta_x} + (-1)^p q^{N-\frac{1}{2}} e^{-x} e^{(1-p)g_s \theta_x} Z_A^{f_2}(x; p) = 0; \quad (6.12)$$

which is nothing but the Schrödinger equation written in the variables appropriate for u_2 patch. All other cases can be deduced easily, too.

These tell us that the A-model amplitudes are the same as the B-model amplitudes supporting the mirror symmetry. We will see this explicitly in below. Note that the Z_2 symmetry is the isometry of the resolved conifold and its mirror CY space. It is realized as the relation in the eq. (6.11) among the (anti-)brane amplitude in the A-model on the resolved conifold and it should also be the case for the amplitude in the mirror B-model. Furthermore, it is well known that the amplitudes in the B-model behave like a wavefunction. Our computation clearly shows that the A-model amplitudes have the properties of the wavefunction, just like the amplitudes in the B-model.

Chern-Simons theory vs. topological vertex vs. DV matrix model

The A-model topological open string field theory on the deformed conifold becomes the $U(N)$ Chern-Simons theory on S^3 . On the other hand, it is believed that the A-model topological string theory on the toric Calabi-Yau space can be described by the topological vertex. There is a large N duality between the A-model topological open string theory on Lagrangian branes wrapped on S^3 in the deformed conifold and the A-model topological string theory on the resolved conifold which is related to the former via geometric transition.

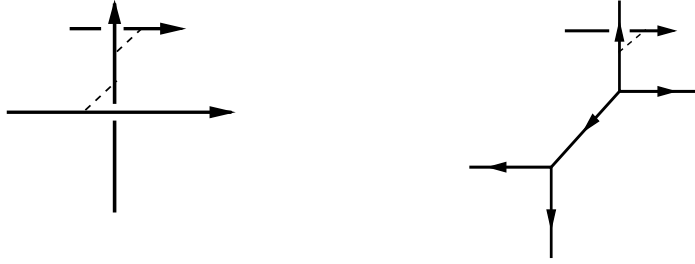


Figure 9: L H S : A-branes on the deformed conifold. R H S : A-branes on the resolved conifold after the geometric transition

We can see from eq.s (3.21) and (3.22) that the knot invariants of the unknot in Chem-Simons theory given in eq.s (2.24) and (2.27) are identical with the amplitude of non-cocompact (anti-)branes inserted at the external leg v_2 with $p = 0$ and $r = g_s N = 2$:

$$hZ(U;V) i_{S^3} = Z_A^{f_2} V; r = \frac{1}{2} g_s N; p = 0; \quad hZ^{-1}(U;V) i_{S^3} = Z_A^{f_2} V; r = \frac{1}{2} g_s N; p = 0;$$

This correspondence between the Chem-Simons knot invariants and the amplitudes at the leg v_2 is pictorially manifest from Fig. 9. We can also find a complete agreement for the knot invariants at a different framing in Chem-Simons theory by taking a suitable framing and an appropriate assignment of the position modulus r in topological vertex.

In the previous sections we computed the amplitudes of a non-cocompact brane in the A-model and the B-model, independently. In the B-model we obtained the amplitude from the large N dual DV matrix model. After an appropriate normalization, the B-model amplitude of a non-cocompact brane inserted at P^1 is given by the determinant expression. Again we see that there is a similar correspondence between the amplitudes in the DV matrix model and those in topological vertex. As alluded earlier, it is clear from the Schrödinger equation which they satisfy. More precisely, if we use the ‘normalized’ expression in DV matrix model, we can see that⁶

$$\begin{aligned} \frac{D \det(e^w - U)}{\det(e^w - U)} &= Z_A^{f_2} (x = w - g_s N + i; p = 1); \\ \frac{D \det(e^w - U)}{\det(e^w)} &= Z_A^{f_2} (x = w - g_s N + i; p = 1); \end{aligned} \quad (6.13)$$

As was shown in (5.17), the unnormalized amplitude satisfies the Schrödinger equation coming from the curve equation $H(x; y) = 0$ in (2.9), which is another representation of the curve in the same u_2 -patch. But this curve equation is related by a suitable framing change and rescaling from our choice of coordinates for the u_2 -patch, which explains the rescaling in the B-model amplitude for the complete agreement with the topological vertex result at the v_2 leg (or u_2 -patch in the corresponding Riemann surface) with framing change. After this identification, we can obtain all the other amplitudes of non-cocompact branes in different patch by suitable $SL(2; \mathbb{Z})$ transformations.

⁶There was an observation [28] that there is a discrepancy between the results from melting crystal model, which agrees with topological vertex, and those from DV matrix model. This is just framing difference between branes on the u_2 -patch coming from DV matrix model and the one from the melting crystal model.

Acknowledgments

The work of S. H. was supported in part by grant No. R01-2004-000-10651-0 from the Basic Research Program of the Korea Science and Engineering Foundation (KOSEF) and by the Science Research Center Program of the Korea Science and Engineering Foundation through the Center for Quantum Spacetime (CQUeST) of Sogang University with grant number R11-2005-021. The work of S.-H. Y. was supported by the Korea Research Foundation Grant KRF-2005-070-C00030.

A Schur functions

In this appendix we present various properties and formulae of Schur functions, which are used in the computation of the topological vertex. Although most of them are just the summary of well-known results [29], one useful identity is presented with a proof, which does not seem to be written down explicitly in the literatures.

Schur functions for a partition $\lambda = (1^j; 2^{j-1}; \dots)$ may be defined as

$$s(\mathbf{x}_i) = s(\mathbf{x}_1; \dots; \mathbf{x}_N) = \frac{\det x_j^{i+N-i}}{\det x_j^{N-i}}; \quad (\text{A.1})$$

which can also be represented in terms of elementary or completely symmetric functions as

$$s(\mathbf{x}_i) = \det(e_{i-i+j}) = \det(h_{i-i+j}); \quad (\text{A.2})$$

These symmetric functions h_n and e_n can be defined as

$$\begin{aligned} \prod_{i=1}^N (1 - x_i t)^{-1} &= \sum_{n=0}^{\infty} t^n h_n(\mathbf{x}_i); \\ \prod_{i=1}^N (1 + x_i t)^{-1} &= \sum_{n=0}^{\infty} t^n e_n(\mathbf{x}_i); \end{aligned} \quad (\text{A.3})$$

Note that s is homogeneous of degree j . For the explicit expression of Schur functions relevant to our cases, it is convenient to introduce the content $c(a)$, and the hook-length $h(a)$, at the position $a = (i; j)$ of a Young diagram, which are defined by

$$c(a) = j - i; \quad h(a) = i + \frac{t}{j} - i - j + 1;$$

These $c(a)$ and $h(a)$ satisfy

$$\sum_{a2}^X c(a) = n(t) \quad n(t) = \frac{1}{2} \sum_{i=1}^{\frac{d(t)}{2}} i(i - 2i + 1) = \frac{1}{2}; \quad \sum_{a2}^X h(a) = \frac{1}{2} + 2n(t) + j(j-1); \quad (\text{A.4})$$

where $d(t)$ denotes the number of rows for the given Young diagram. By specializing $x_i = q^{i-1}$, with the formula in [29], one can derive

$$s(q^{i-\frac{1}{2}}) = q^{n(t) - \frac{1}{2}j(j-1)} \prod_{a2}^Y \frac{1 - q^{N-c(a)}}{1 - q^{h(a)}} = q^{\frac{j-j}{2}N} \prod_{a2}^Y \frac{q^{\frac{N}{2} + \frac{1}{2}c(a)} - q^{\frac{N}{2} - \frac{1}{2}c(a)}}{q^{\frac{1}{2}h(a)} - q^{\frac{1}{2}h(a)}}, \quad (\text{A.5})$$

where $n(\) = \prod_{i=1}^{d(\)} (i-1)$. Note that $q^{\frac{N}{2}j} s_{\text{ }}(q^{i+1=2})$ is nothing but the quantum dimension or the knot invariants for the unknots. The given form is efficient to get the explicit expression of the quantum dimension for a Young diagram of the small number of boxes.

Using another identities given in [29]

$$\begin{aligned} \underset{a2}{\text{Y}} \quad (1 - t^{h(a)}) &= \frac{Q_{d(\)} Q_{d(\)+i-i}}{Q_{\underset{1 \leq j \leq d(\)}{\text{Y}} (1 - t^{i-j})} (1 - t^{i-j+i})}; \\ \underset{a2}{\text{Y}} \quad (1 - t^{N+c(a)}) &= \frac{Q_{\underset{i=1 \leq k \leq i+1}{\text{Y}}}}{(1 - t^{N+k})}; \end{aligned} \quad (\text{A.6})$$

one can get the form of the quantum dimension given in [2]

$$\begin{aligned} s_{\text{ }}(q^{\frac{N}{2}-i+\frac{1}{2}}) = \dim_q &= \underset{1 \leq j \leq d(\)}{\text{Y}} \frac{Q_{\underset{i-j-j-i}{\text{Y}}}}{Q_{\underset{i=1}{\text{Y}} \underset{k=1}{\text{Y}} \underset{i+1}{\text{Y}}}} \frac{Q_{\underset{i-i+1}{\text{Y}}}}{Q_{\underset{i=1}{\text{Y}} \underset{k=1}{\text{Y}} \underset{i+1}{\text{Y}}}}; \\ &= \underset{1 \leq j \leq d(\)}{\text{Y}} \frac{Q_{\underset{i-j-j-i}{\text{Y}}}}{Q_{\underset{i-j-i}{\text{Y}}}} \frac{Q_{\underset{i-i+1}{\text{Y}}}}{Q_{\underset{i=1}{\text{Y}} \underset{k=1}{\text{Y}} \underset{i+1}{\text{Y}}}}; \end{aligned} \quad (\text{A.7})$$

where $[k] = q^{\frac{k}{2}} - q^{-\frac{k}{2}}$ and $[k]_{q^N} = q^{\frac{N}{2}+\frac{k}{2}} - q^{\frac{N}{2}-\frac{k}{2}}$.

Skew Schur functions can be introduced as

$$s_{\text{ }} = \underset{X}{\text{c}} \underset{S}{\text{ }}; \quad (\text{A.8})$$

where the 'tensor product coefficient' c are integers defined by $s_{\text{ }}s_{\text{ }} = \underset{P}{\text{c}} s_{\text{ }}s_{\text{ }}$. Note that $s_{\text{ }}$ is a homogeneous function of degree $j-j-j-j$ and Schur functions can be understood as a special case of skew Schur functions since $s_{\text{ }} = s_{\text{ }}$. As in [9], $s_{\text{ }}(q^+)$ represents a skew Schur function of infinite number of variables with the specialized $x_i = q^{i-i+1=2}$ ($i = 1, 2, \dots$), which can be understood as taking $N \rightarrow 1$ in the case of the finite number of x_i . In particular, $s_{\text{ }}(q)$ can be written explicitly as

$$s_{\text{ }}(q) = q^{n(\) - \frac{1}{2}j-j} \underset{a2}{\text{Y}} \frac{1}{1 - q^{h(a)}}; \quad (\text{A.9})$$

which leads to

$$s_{\text{ }}(q) = q^{-2} s_{\text{ }}(q); \quad (\text{A.10})$$

By analytic continuation one may see

$$s_{\text{ }}(q) = (-1)^j s_{\text{ }}(q); \quad (\text{A.11})$$

The definition of Schur functions as a ratio of determinants given in (A.1) leads to the following identity for a finite number of variables $x_i = q^{N-i}; q^{i+N-i}$ ($i = 1, 2, \dots, N$)

$$s_{\text{ }}(q^{N-i}) s_{\text{ }}(q^{i+N-i}) = s_{\text{ }}(q^{i+N-i}) s_{\text{ }}(q^{N-i}); \quad (\text{A.12})$$

which gives us in the limit of $N \rightarrow 1$

$$s_{\text{ }}(q) s_{\text{ }}(q^+) = s_{\text{ }}(q^+) s_{\text{ }}(q); \quad (\text{A.13})$$

Another useful formulae for skew Schur functions [29]:

$$\sum_{\lambda} s_{\lambda}(x) s_{\lambda}(y) = \sum_{\substack{i,j \\ i \neq j}} \frac{1}{1 - x_i y_j} \sum_{\lambda} s_{\lambda}(x) s_{\lambda}(y); \quad (\text{A.14})$$

$$\sum_{\lambda} s_{\lambda^t}(x) s_{\lambda^t}(y) = \sum_{\substack{i,j \\ i \neq j}} (1 + x_i y_j) \sum_{\lambda} s_{\lambda^t}(x) s_{\lambda^t}(y); \quad (\text{A.15})$$

Now, we will derive a useful formula for the topological vertex calculations.

Proposition: The following identity holds

$$\sum_{\lambda} s_{\lambda}(x) = \sum_{\lambda} s_{\lambda}(x; y) s_{\lambda^t}(y); \quad (\text{A.16})$$

Proof: Let us start from the following identity (see, [29])

$$\sum_{\lambda} s_{\lambda}(x; y) = \sum_{\lambda} s_{\lambda}(x) s_{\lambda}(y) = \sum_{\lambda} c_{\lambda} s_{\lambda}(x) s_{\lambda}(y);$$

Multiplying $s_{\lambda}(y)$ and summing over λ , one gets

$$\begin{aligned} \sum_{\lambda} s_{\lambda}(x; y) s_{\lambda}(y) &= \sum_{\lambda} c_{\lambda} s_{\lambda}(x) s_{\lambda}(y) s_{\lambda}(y) \\ &= \sum_{\lambda} s_{\lambda}(y) s_{\lambda}(y) \sum_{\lambda} s_{\lambda}(x) s_{\lambda}(y); \end{aligned}$$

Using eqs (A.14) and (A.15), one gets

$$\sum_{\lambda} s_{\lambda}(y) s_{\lambda}(y) = \sum_{\lambda} s_{\lambda}(y) s_{\lambda^t}(y);$$

which leads to

$$\begin{aligned} \sum_{\lambda} s_{\lambda}(x) s_{\lambda}(y) &= \sum_{\lambda} s_{\lambda}(x; y) s_{\lambda}(y) \sum_{\lambda} s_{\lambda}(y) s_{\lambda^t}(y); \\ &= \sum_{\lambda} s_{\lambda}(x; y) s_{\lambda^t}(y) \sum_{\lambda} s_{\lambda}(y); \end{aligned}$$

Since Schur functions form a \mathbb{Z} -basis for symmetric functions, the coefficient of $s_{\lambda}(x)$ in the above equation should be identical. So, the proposition is proved.

As an application of the above proposition, let us take

$$\begin{aligned} x_1 &= q^{\frac{1}{2}}; \quad x_2 = q^{\frac{3}{2}}; \quad \dots; \quad x_N = q^{N + \frac{1}{2}}; \quad x_{N+1} = x_{N+2} = \dots = 0; \\ y_i &= q^{N - i + \frac{1}{2}}; \quad i = 1; 2; 3; \quad \dots; \end{aligned}$$

which gives us $s_{\lambda}(x; y) = s_{\lambda}(q)$. Then, we can see that

Corollary:

$$s_{\lambda}(q^{-i + \frac{1}{2}}) s_{\lambda}(q^{\frac{1}{2}}; \dots; q^{N + \frac{1}{2}}) = \sum_{\lambda} s_{\lambda}(q) s_{\lambda^t}(q^N q); \quad (\text{A.17})$$

Now, we present the skew-Schur function representation of topological vertex, which is used in section 3. Up (1) Hopf link invariants, W , which are basic ingredients for the construction of topological vertex, can be written by skew Schur functions as

$$\begin{aligned} W(q) &= q^{-2} C_t(q) = q^{-2+} \stackrel{X}{=} s_{t-}(q) s_{t-}(q) = s_t(q) s_{t-}(q^+); \\ W(q) &= C_t(q) = s_t(q); \end{aligned} \quad (\text{A.18})$$

Then, topological vertex is given in terms of skew Schur functions by [9][30][31]

$$C_t(q) = C_{t-}(q) = C_{t-}(q) = q^{-2+} \stackrel{X}{=} s_{t-}(q) s_{t-}(q^+) s_{t-}(q^{t+}); \quad (\text{A.19})$$

Note that the Z_2 and Z_3 symmetry of the topological vertex implies the existence of corresponding identities inherited from these symmetries in skew-Schur functions.

References

- [1] K. Hori et al, "Mirror symmetry," Clay Mathematics Monographs, 2003; vol. 1.
- [2] M. Mariño, "Chem-Simons theory and topological strings," [arXiv:hep-th/0406005].
- [3] M. Mariño, "Les Houches lectures on matrix models and topological strings," [arXiv:hep-th/0410165].
- [4] A. Neitzke and C. Vafa, "Topological strings and their physical applications," [arXiv:hep-th/0410178].
- [5] E. Witten, "Chem-Simons Gauge Theory As A String Theory," Prog. Math. 133 (1995) 637 [arXiv:hep-th/9207094].
- [6] R. Gopakumar and C. Vafa, "On the gauge theory/geometry correspondence," Adv. Theor. Math. Phys. 3 (1999) 1415 [arXiv:hep-th/9811131].
- [7] N. Berkovits, H. Ooguri and C. Vafa, "On the worldsheet derivation of large N dualities for the superstring," Commun. Math. Phys. 252, 259 (2004) [arXiv:hep-th/0310118].
- [8] M. Aganagic, A. Kleemann, M. Mariño and C. Vafa, "The topological vertex," [arXiv:hep-th/0305132].
- [9] A. Okounkov, N. Reshetikhin and C. Vafa, "Quantum Calabi-Yau and classical crystals," [arXiv:hep-th/0309208].
- [10] T. Okuda, "Derivation of Calabi-Yau crystals from Chem-Simons gauge theory," JHEP 0503 (2005) 047 [arXiv:hep-th/0409270].
- [11] N. Saulina and C. Vafa, "D-branes as defects in the Calabi-Yau crystal," [arXiv:hep-th/0404246].
- [12] M. Aganagic, R. Dijkgraaf, A. Kleemann, M. Mariño and C. Vafa, "Topological strings and integrable hierarchies," Commun. Math. Phys. 261, 451 (2006) [arXiv:hep-th/0312085].

[13] R. Dijkgraaf and C. Vafa, "Matrix models, topological strings, and supersymmetric gauge theories," *Nucl. Phys. B* 644, 3 (2002) [[arXiv:hep-th/0206255](#)]; R. Dijkgraaf and C. Vafa, "On geometry and matrix models," *Nucl. Phys. B* 644, 21 (2002) [[arXiv:hep-th/0207106](#)]; R. Dijkgraaf and C. Vafa, "A perturbative window into non-perturbative physics," [[arXiv:hep-th/0208048](#)].

[14] A. K. Kashani-Poor, "The wave function behavior of the open topological string partition function on the conifold," [[arXiv:hep-th/0606112](#)].

[15] C. Vafa, "Superstrings and topological strings at large N ," *J. Math. Phys.* 42 (2001) 2798 [[arXiv:hep-th/0008142](#)].

[16] K. Hori and C. Vafa, "Mirror symmetry," [[arXiv:hep-th/0002222](#)]; K. Hori, A. Iqbal and C. Vafa, "D-branes and mirror symmetry," [[arXiv:hep-th/0005247](#)].

[17] E. Witten, "Phases of $N = 2$ theories in two dimensions," *Nucl. Phys. B* 403, 159 (1993) [[arXiv:hep-th/9301042](#)].

[18] M. Aganagic, A. Kleemann, M. Mariño and C. Vafa, "Matrix models as a mirror of Chern-Simons theory," *JHEP* 0402, 010 (2004) [[arXiv:hep-th/0211098](#)].

[19] R. Gopakumar and C. Vafa, "M-theory and topological strings. I," [[arXiv:hep-th/9809187](#)]; "M-theory and topological strings. II," [[arXiv:hep-th/9812127](#)].

[20] H. Ooguri and C. Vafa, "Knot invariants and topological strings," *Nucl. Phys. B* 577, 419 (2000) [[arXiv:hep-th/9912123](#)].

[21] E. Witten, "Quantum field theory and the Jones polynomial," *Commun. Math. Phys.* 121 (1989) 351.

[22] M. Aganagic and C. Vafa, "Mirror symmetry, D-branes and counting holomorphic discs," [[arXiv:hep-th/0012041](#)].

[23] M. Aganagic, A. Kleemann and C. Vafa, "Disk instantons, mirror symmetry and the duality web," *Z. Naturforsch. A* 57, 1 (2002) [[arXiv:hep-th/0105045](#)].

[24] M. Mariño and C. Vafa, "Framed knots at large N ," [[arXiv:hep-th/0108064](#)]; J. M. F. Labastida, M. Mariño and C. Vafa, "Knots, links and branes at large N ," *JHEP* 0011, 007 (2000) [[arXiv:hep-th/0010102](#)].

[25] N. Halmagyi, A. S. Sorkin and P. Sulkowski, "Knot invariants and Calabi-Yau crystals," *JHEP* 0601 (2006) 040 [[arXiv:hep-th/0506230](#)].

[26] M. Bershadsky, S. Cecotti, H. Ooguri and C. Vafa, "Kodaira-Spencer theory of gravity and exact results for quantum string amplitudes," *Commun. Math. Phys.* 165, 311 (1994) [[arXiv:hep-th/9309140](#)].

[27] M. Tierz, "Soft matrix models and Chern-Simons partition functions," *Mod. Phys. Lett. A* 19, 1365 (2004) [[arXiv:hep-th/0212128](#)].

[28] K. Okuyama, "D-brane amplitudes in topological string on conifold," [[arXiv:hep-th/0606048](#)].

[29] I.G. Macdonald, "Symmetric functions and Hall polynomials," 2nd Ed. Oxford U. Press.

[30] T. Eguchi and H. Kanno, "Topological strings and Nekrasov's formulas," JHEP 0312 (2003) 006 [[arXiv:hep-th/0310235](#)].

[31] T. J. Hollowood, A. Iqbal and C. Vafa, "Matrix models, geometric engineering and elliptic genera," [[arXiv:hep-th/0310272](#)].